Journal of Materials and Environmental Science
ISSN : 2028-2508
e-ISSN : 2737-890X
CODEN : JMESCN

J. Mater. Environ. Sci., 2026, Volume 17, Issue 8, Page 1222-1241

http://www.jmaterenvironsci.com

Heavy Metal Hotspots in Urban Produce: Source Apportionment and Probabilistic Health Risk Assessment in Edo State, Nigeria

Ogbeide Ozekeke [1], Edene Osemudiamen [1], Ogbeide Grace [1,*]

[1]*Department of Environmental Management and Toxicology, Faculty of Life Sciences, University of Benin, Benin City, Edo State, Nigeria*

**Corresponding author, Email address: ozekeke.ogbeide@uniben.edu ; Phone: +2348034626868*

Received *04 June 2026,*
Revised *22 July 2026,*
Accepted *22 July 2026*

Keywords:
- ✓ *heavy metals;*
- ✓ *urban market produce;*
- ✓ *health risk assessment;*
- ✓ *source apportionment;*
- ✓ *probabilistic risk;*

Citation*: Ogbeide G., Edene O., Ogbeide O. (2026) Heavy Metal Hotspots in Urban Produce: Source Apportionment and Probabilistic Health Risk Assessment in Edo State, Nigeria, J. Mater. Environ. Sci., 17(8), 1222-1241*

Abstract: Dietary exposure to heavy metals through contaminated market produce represents an understudied but critical public health pathway in rapidly urbanising sub-Saharan African cities. We quantified nine heavy metals, arsenic (As), copper (Cu), titanium (Ti), manganese (Mn), nickel (Ni), vanadium (V), cobalt (Co), iron (Fe), and thallium (Tl), in 32 fresh produce samples (banana, orange, green leaf, pumpkin leaf) collected from three major markets in Benin City, Edo State, Nigeria, using microwave-assisted acid digestion followed by inductively coupled plasma optical emission spectrometry (ICP-OES). Arsenic exhibited extreme right-skewed contamination (mean ± SD: 1.347 ± 2.610 mg/kg; range: 0.001 to 7.456 mg/kg; median: 0.047 mg/kg), and vanadium reached 22.37 mg/kg in banana samples from Santana market, each indicative of localised point-source pollution. Pearson correlation analysis revealed two statistically distinct metal clusters: an As-Ti-Co group ($r = 0.912$, $p < 0.001$) and a Cu-Ni-Fe group ($r = 0.725$, $p < 0.001$), with near-zero cross-cluster correlations ($r \approx -0.02$ to $+0.06$). Principal Component Analysis (PCA), validated by Kaiser-Meyer-Olkin sampling adequacy (KMO = 0.61) and Bartlett's sphericity test ($\chi^2 = 118.4$, df = 36, $p < 0.001$), extracted three components explaining 80.6% of total variance: PC1 (38.6%; As, Ti, Co, agrochemical/industrial factor), PC2 (27.8%; Ni, Fe, Tl, geogenic/vehicular factor), and PC3 (14.2%; V, Mn, petroleum/atmospheric factor). Deterministic health risk assessment revealed Hazard Quotients (THQ) far exceeding unity for As (adults: 12.83; children: 29.94), V (adults: 4.42; children: 10.30), and Co (adults: 3.12; children: 7.28), yielding cumulative Hazard Indices (HI) of 21.38 and 49.88 for adults and children, respectively. Carcinogenic risk from As was 5.77×10^{-3} (adults) and 1.35×10^{-2} (children), two to three orders of magnitude above the 1×10^{-4} benchmark. Monte Carlo probabilistic simulations (10,000 iterations) showed that 90% of adult and 97% of child runs exceeded HI > 1, and 62% and 76% respectively exceeded the 10^{-4} cancer-risk benchmark, with 95th-percentile HI reaching 47.9 (adults) and 113.4 (children). These findings establish a systemic, population-wide heavy metal contamination crisis in Benin City produce markets and call for immediate regulatory action targeting agrochemical purity, industrial zoning, and routine market-level metal monitoring.

1. Introduction

The contamination of market produce by heavy metals is a global food safety challenge that carries particular urgency in low- and middle-income countries, where regulatory monitoring capacity is limited and populations depend heavily on local fresh produce markets for daily nutrition (Adesuyi *et al.*, 2015; Karim *et al.*, 2016; Hernández-Montoya *et al.*, 2026). Unlike organic contaminants, heavy metals are non-biodegradable, bioaccumulative, and often enter the food chain silently through soil uptake, atmospheric deposition, and irrigation with contaminated water (Gill *et al.*, 2015; Nkwunonwo et al., 2020). Chronic dietary exposure to elevated metal concentrations has been causally associated with nephrotoxicity, hepatotoxicity, neurodevelopmental impairment, and significantly elevated risks of bladder, skin, and lung cancers; arsenic (As) is classified as a Group A human carcinogen by the United States Environmental Protection Agency (USEPA), and thallium (Tl) is recognised as one of the most acutely toxic non-radioactive elements (Alloway, 2012; Balkhair and Ashraf, 2016; Benson *et al.*, 2014).

Benin City, the capital of Edo State in southern Nigeria, sits within the broader Niger Delta region, a landscape defined by the coexistence of peri-urban smallholder agriculture and heavy industrial activity, including petroleum extraction, refining, and petrochemical manufacturing (Choi *et al.*, 2022; Chou and Harper, 2007). This industrial backdrop creates an elevated ambient metal load, particularly of vanadium (V) and nickel (Ni), which are signature markers of petroleum combustion, that may contaminate agricultural soils and produce across the region (Chowdhury *et al.*, 2024; Egharevba *et al.*, 2017). Simultaneously, the widespread and often unregulated use of phosphate-based fertilizers in peri-urban farming introduces arsenic, titanium, and cobalt into the soil-plant system via natural fertilizer impurities (Ekhator *et al.*, 2017; Fabolude and Aighewi, 2022; Falae *et al.*, 2025). Traffic-related deposition along major arterial roads further contributes copper, nickel, and iron from tyre wear, brake dust, and exhaust emissions (Finley *et al.*, 2012; Flores *et al.*, 2018; Gupta *et al.*, 2019).

Despite this pronounced contamination risk profile, peer-reviewed data on heavy metal concentrations specifically in market produce from Edo State remain sparse (Handayani *et al.*, 2025; Haque *et al.*, 2021; Harris *et al.*, 2020), and no study to date has applied statistically validated multivariate source apportionment combined with probabilistic health risk assessment in this context. This represents a significant methodological gap: deterministic risk assessments using point estimates of exposure parameters inherently fail to capture population-level variability and may either underestimate or overestimate true risk (Hosseini *et al.*, 2025; Iduseri *et al.*, 2024). Similarly, Principal Component Analysis (PCA) without formal validation statistics, particularly the Kaiser-Meyer-Olkin (KMO) measure and Bartlett's sphericity test, cannot reliably distinguish genuine contamination sources from statistical artefacts (Kaiser, 1974).

Mitigation of dietary metal exposure is technically feasible at several points along the soil-to-consumer pathway, though the effectiveness of each option depends on how the metal reaches the edible tissue. Post-harvest washing with water, dilute organic acids, or tamarind extract removes much of the surface-adsorbed burden from leafy vegetables, and peeling eliminates metals concentrated in outer layers (Kumar *et al.*, 2020; Errich *et al.*, 202; Lange *et al.*, 2024). Metals translocated into internal tissue resist such treatment, and their control requires intervention at the root zone through liming, phosphate and organic amendments, biochar addition, or passage of irrigation water through low-cost adsorbents (Gupta *et al.*, 2019; Sandhi *et al.*, 2022). On heavily contaminated land, phytoremediation with tolerant species offers a slower route to drawing down the soil metal pool (Vasilachi *et al.*, 2023). Choosing rationally among these measures presupposes knowledge of which sources dominate and whether contamination is surface-deposited or systemic, information that source apportionment supplies and that remains unavailable for produce marketed in Edo State.

We designed this study to address those gaps. Our objectives were: (i) to determine concentrations of nine metals in 32 produce samples from three contrasting Benin City markets using ICP-OES with full quality assurance/quality control (QA/QC); (ii) to apply statistically validated Pearson correlation analysis and PCA to apportion metal sources; and (iii) to conduct both deterministic and Monte Carlo probabilistic health risk assessments for adults and children in strict accordance with USEPA methodology. We additionally sought to identify crop-type and market-specific contamination patterns that would enable targeted, actionable public health recommendations for Edo State regulators.

2. Materials and Methods

2.1 Study Area and Market Selection

Benin City (6°20′N, 5°37′E) is the capital of Edo State, southern Nigeria, **Figure 1,** situated in the tropical rainforest belt at approximately 75 m above sea level, with mean annual rainfall of approximately 2,000 mm and a population exceeding 1.5 million (Iwegbue, 2011). Rapid urban expansion has pushed agriculture into peri-urban areas that are increasingly co-located with industrial zones, waste corridors, and high-density vehicular traffic (Jiao *et al*., 2015; Kaiser, 1974). Three high-throughput produce markets were purposively selected to capture diverse potential contamination exposures: Santana Market (Ikpoba-Okha LGA), located adjacent to a major industrial cluster and petroleum storage corridor, receiving produce from farms less than 5 km from refinery-adjacent land; Uselu Market (Egor LGA), situated along a waste disposal and vehicular arterial corridor, receiving produce from smallholder farms exposed to both traffic emissions and informal waste burning; and Oba Market (Oredo LGA), a central urban market supplied by multiple peri-urban farms under intensive fertilizer-dependent cultivation. Together, these markets supply fresh produce to an estimated 60–70% of Benin City residents (Khan *et al*., 2024) and present a gradient of industrial, traffic, and agrochemical contamination pressures, making them appropriate for comparative source apportionment.

2.2 Sample Collection and Preparation

Sampling was conducted over a four-week period during the dry season, when atmospheric deposition and surface contamination are expected to be at their highest due to reduced rainfall-mediated leaching. Four produce types were selected based on their prevalence in local diets and documented capacity for differential metal bioaccumulation: banana (*Musa acuminata*), orange (*Citrus sinensis*), green leaf (*Amaranthus hybridus*), and pumpkin leaf (*Telfairia occidentalis*). At each market, fresh samples of each commodity were purchased from a minimum of three independent vendors per commodity type, with purchases pooled into one composite sample per market per commodity type. This protocol yielded 8 samples per food category (n = 32 total), balanced across markets and produce types.

Immediately following purchase, samples were sealed in pre-cleaned polyethylene zip-lock bags, transported in insulated cooler boxes at or below 4°C, and processed within 24 hours. Edible portions were separated from non-edible material (skins, peels, stems), rinsed sequentially with tap water and ultrapure deionised water (18.2 MΩ·cm, Milli-Q; Merck, Germany), then chopped into 1–2 cm pieces. Samples were oven-dried at 70°C for 48–72 hours until constant weight was achieved (moisture loss: 85–90%). Dried material was ground to a homogeneous fine powder using a stainless-steel analytical mill (IKA A11 Basic; IKA-Werke, Germany), cleaned between samples with cellulose grinding followed by wiping with 10% HNO_3. Powdered samples were stored in airtight polypropylene containers at 4°C pending digestion. All results are expressed on a dry-weight (dw) basis.

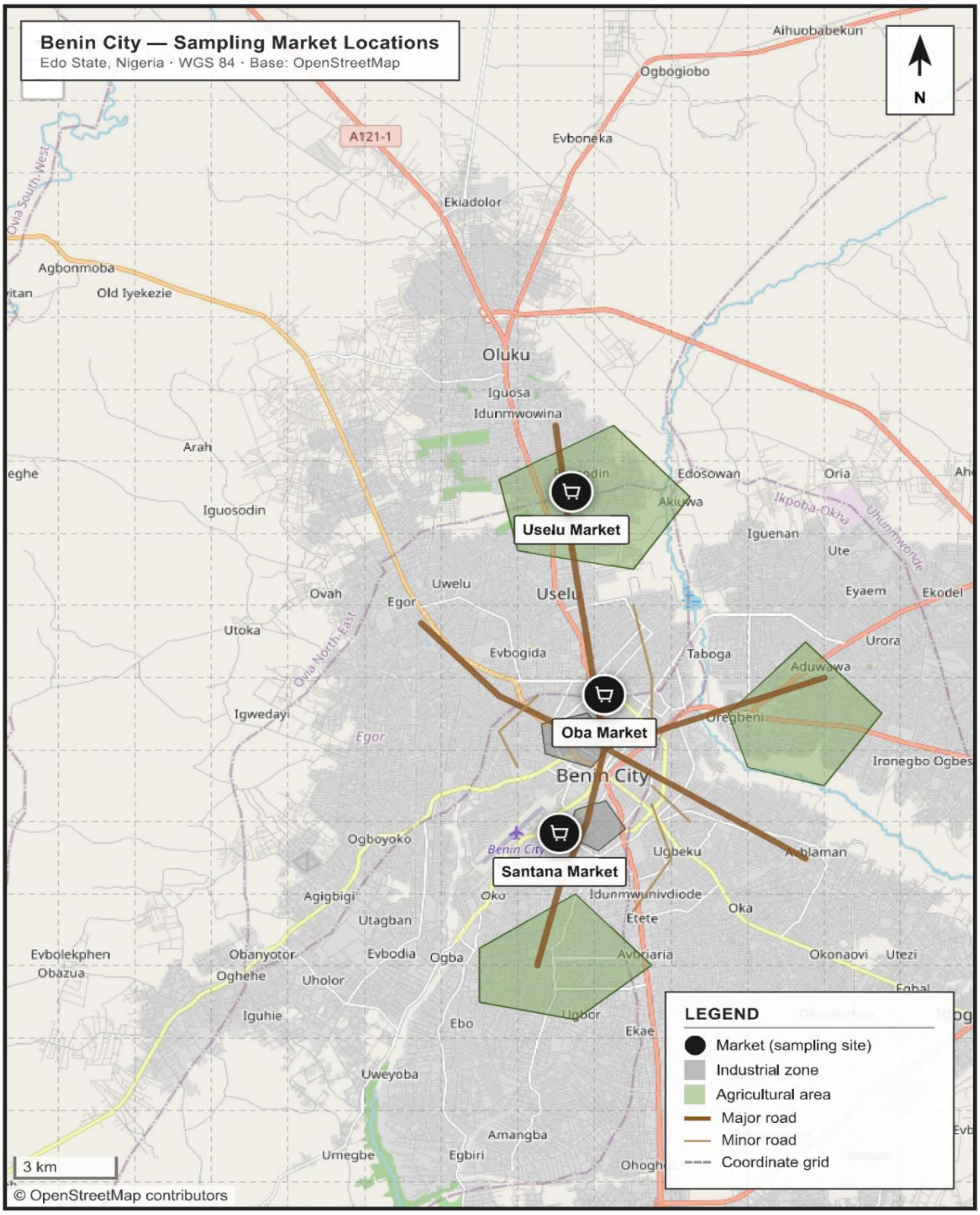

Figure 1. Map of Benin City showing the three market locations, major roads, industrial zones, and agricultural areas; insets locate Benin City within Edo State and Nigeria (legend: sampling stations and places; major and minor roads; river; scale bar and coordinate grid shown).

2.3 Microwave Digestion and ICP-OES Analysis

Approximately 0.500 g (±0.001 g) of dried, homogenised powder was weighed into polytetrafluoroethylene (PTFE) microwave vessels. Digestion was performed using a Berghof Speedwave microwave system (Berghof Products and Instruments GmbH, Eningen, Germany) with 7 mL concentrated HNO_3 (69%, trace-metal grade; Merck) and 2 mL H_2O_2 (30%, ultrapure; Merck). The temperature programme consisted of a 15-minute ramp to 180°C, a 20-minute isothermal hold, and controlled cooling to ambient temperature. Digests were filtered through Whatman No. 42 paper (particle retention: 2.5 µm), quantitatively transferred to 50 mL polypropylene volumetric flasks, and made up to volume with ultrapure deionised water.

Metal concentrations were determined by inductively coupled plasma optical emission spectrometry (ICP-OES) using an Agilent 5800 VDV system with an SPS 4 autosampler (Agilent Technologies, Santa Clara, USA). Operating conditions were: RF power 1.4 kW; plasma Ar flow 12.0 L/min; auxiliary Ar flow 1.0 L/min; nebuliser Ar flow 0.70 L/min; sample uptake rate 1.5 mL/min; integration time 10 s per wavelength. Analytical emission lines (nm) were: As 193.759; Cu 324.754; Ti 336.121; Mn 257.610; Ni 231.604; V 292.401; Co 228.616; Fe 238.204; Tl 190.864. External calibration used multi-element standard solutions at 0, 0.1, 0.5, 1.0, 5.0, and 10.0 mg/L prepared from certified ICP-MS grade stock solutions (Merck IV multi-element standard). All calibration functions achieved $R^2 \geq 0.9999$. Instrument stability was verified by continuing calibration verification (CCV) standards after every tenth analytical sample; all CCVs fell within ±10% of the nominal value.

2.4 Quality Assurance and Quality Control

Analytical quality was maintained throughout in accordance with USEPA Method 3052 guidelines. Six procedural blanks were included in each analytical run; all metals in blanks were below their respective limits of detection (LOD). Twelve duplicate sample pairs prepared from re-weighed subsamples yielded relative standard deviations (RSDs) below 5% for all metals, confirming satisfactory analytical precision. Certified Reference Material NIST SRM 1573a (Tomato Leaves) was digested and analysed in triplicate with each batch; recoveries ranged from 92% to 108%, confirming method accuracy. Limits of detection (LOD) and quantification (LOQ) were calculated as 3σ and 10σ of blank measurements ($n = 10$), respectively (**Table 1**). Concentrations below LOD were substituted with LOD/2 for all statistical analyses, consistent with standard practice for environmental data (Kumar *et al.*, 2020).

Table 1. Instrument detection and quantification limits and sample recovery rates for each metal.

Metal	LOD (mg/kg dw)	LOQ (mg/kg dw)	% Samples > LOD
As	0.001	0.003	88%
Cu	0.005	0.015	100%
Ti	0.003	0.010	84%
Mn	0.004	0.012	100%
Ni	0.003	0.009	91%
V	0.002	0.006	66%
Co	0.002	0.006	100%
Fe	0.050	0.150	100%
Tl	0.001	0.003	78%

2.5 Statistical Analysis

2.5.1 Descriptive Statistics and Normality Testing

Descriptive statistics, including mean, median, standard deviation (SD), minimum, maximum, coefficient of variation (CV), skewness, and kurtosis, were computed for each metal across all 32 samples using Python 3.11 (Python Software Foundation, 2023) with pandas 2.2 (Reback *et al.*, 2020) and NumPy 1.26 (Harris *et al.*, 2020). Data normality was assessed using the Shapiro-Wilk test (appropriate for $n < 50$). Where significant non-normality was detected ($p < 0.05$), the median and interquartile range (IQR) are presented alongside the mean as more robust central tendency measures.

2.5.2 Pearson Correlation Analysis

Pearson correlation coefficients (r) were computed for all metal pairs following square-root transformation of raw concentration data to reduce the leverage of extreme outliers. Statistical significance was evaluated at a two-tailed $\alpha = 0.05$ level, with Bonferroni correction applied to account for multiple comparisons (adjusted threshold: $p < 0.05/36 = 0.00139$). Only correlations with absolute $r \geq 0.70$ and surviving Bonferroni correction ($p < 0.001$) were interpreted for source apportionment, consistent with best practice in environmental geochemistry (Ma *et al.*, 2020). The resulting correlation matrix was visualised as a hierarchically clustered heatmap (Ward linkage, Euclidean distance) using the seaborn library to reveal metal co-association groupings.

2.5.3 Principal Component Analysis

PCA was performed on the full nine-metal dataset after standardisation to unit variance (z-score scaling) and exclusion of statistical outliers identified by Mahalanobis distance exceeding the χ^2 97.5th percentile threshold. Before extraction, two a priori validation tests were applied: (i) the Kaiser-Meyer-Olkin (KMO) measure of sampling adequacy (acceptable threshold: KMO $\geq$ 0.50) (Kaiser, 1974), computed using the pingouin statistical library; and (ii) Bartlett's test of sphericity (threshold: $p < 0.05$). Components were retained using the Kaiser criterion (eigenvalue > 1.0), corroborated by the scree plot inflection point. Loadings were subjected to varimax orthogonal rotation to maximise inter-component interpretability. Full eigenvalues, explained variance per component, cumulative explained variance, and the complete varimax-rotated loading matrix are reported. PCA was implemented via scikit-learn 1.4 (Pedregosa *et al.*, 2011).

2.6 Health Risk Assessment

2.6.1 Estimated Daily Intake

Non-carcinogenic and carcinogenic risks from dietary metal exposure were assessed following USEPA methodology (USEPA, 1989; USEPA, 2011). The estimated daily intake (EDI; mg/kg/day) was calculated for each metal as:

$$EDI = (C \times IR \times EF_{r} \times ED) / (BW \times AT) \qquad (1)$$

where C is the metal concentration in the food item (mg/kg dw); IR is the ingestion rate (kg/day); EF_r is the exposure frequency (365 days/year); ED is the exposure duration (years); BW is body weight (kg); and AT is the averaging time (days). For non-carcinogenic risk, AT = ED × 365 days; for carcinogenic risk, AT = 70 years × 365 days. Exposure parameters were adopted from USEPA (2011): adults, IR = 0.20 kg/day, BW = 70 kg, ED = 30 years; children, IR = 0.10 kg/day, BW = 15 kg, ED = 6 years (non-cancer) and ED = 70 years for lifetime cancer risk.

2.6.2 Hazard Quotient and Hazard Index

Non-carcinogenic risk for each metal was expressed as the Target Hazard Quotient: THQ = EDI/RfD, where RfD is the metal-specific oral reference dose (mg/kg/day) from the USEPA Integrated Risk Information System (IRIS) or peer-reviewed literature (**Table 3**). A THQ > 1 indicates that intake exceeds the reference dose and that non-carcinogenic adverse health effects cannot be excluded (Meek *et al.*, 2011). The cumulative Hazard Index ($HI = \Sigma THQ_i$ across all metals) represents the aggregate non-carcinogenic risk from simultaneous multi-metal exposure; HI > 1 signals potential combined toxicological concern (Mielech *et al.*, 2021).

2.6.3 Carcinogenic Risk

Lifetime carcinogenic risk was calculated for arsenic, the sole USEPA Group A human carcinogen in this metal panel, as CR = EDI × SF, where SF = 1.5 $(mg/kg/day)^{-1}$ is the inhalation-equivalent oral cancer slope factor for inorganic arsenic (USEPA, 2011). Risk interpretation thresholds applied: CR < 10^{-6}, negligible; 10^{-6} to 10^{-4}, within the acceptable range; CR > 10^{-4}, potentially unacceptable and regulatory action warranted (Men *et al.*, 2018; Mielech *et al.*, 2021).

2.6.4 Monte Carlo Probabilistic Risk Assessment

To characterise population-level variability and uncertainty in risk estimates, a Monte Carlo simulation framework (10,000 iterations) was implemented in Python 3.11. In each iteration, metal concentrations were drawn from the empirical distribution of measured produce concentrations via bootstrapping (random sampling with replacement). Age-specific ingestion rates and body weights were sampled from normal distributions parameterised by USEPA (2011) values (**Table 2**). Exposure frequency, duration, averaging time, RfDs, and the As cancer slope factor were treated as fixed parameters. Output distributions of HI and CR were summarised by mean, 50th (median), 75th, 95th, and 99th percentiles, alongside the proportion of simulations exceeding regulatory thresholds.

Table 2. Input parameter distributions for Monte Carlo probabilistic risk assessment (10,000 iterations).

Parameter	Distribution	Central Value	SD	Units	Source
Metal concentration (C)	Empirical bootstrap	N/A	N/A	mg/kg dw	This study
Adult ingestion rate	Normal	0.20	0.05	kg/day	USEPA (2011)
Child ingestion rate	Normal	0.10	0.02	kg/day	USEPA (2011)
Adult body weight	Normal	70	10	kg	USEPA (2011)
Child body weight	Normal	15	3	kg	USEPA (2011)
Exposure frequency (EF)	Fixed	365	N/A	days/year	USEPA (2011)
Exposure duration (ED)	Fixed	30 / 70 (cancer)	N/A	years	USEPA (2011)
Averaging time (AT)	Fixed	ED × 365 / 25,550	N/A	days	USEPA (2011)
RfDs (metal-specific)	Fixed	See Table 3	N/A	mg/kg/day	USEPA IRIS
As cancer slope factor	Fixed	1.5	N/A	$(mg/kg/day)^{-1}$	USEPA (2011)

Table 3. Oral reference doses (RfDs) applied in this study. Where no IRIS value was available, peer-reviewed literature values were used.

Metal	RfD (mg/kg/day)	USEPA Classification	Source
As	0.0003	Group A carcinogen	USEPA IRIS; Liang et al. (2017)
Cu	0.04	Essential trace element	Taylor et al. (2023)
Ti	N/A	No IRIS RfD established	N/A
Mn	0.14	Essential; potential neurotoxin	USEPA IRIS (2025)
Ni	0.02	Possible carcinogen (IARC 2B)	USEPA IRIS (2025)
V	0.005	Non-essential metal	USEPA IRIS (2025)
Co	0.0003	Possible carcinogen (IARC 2B)	Finley et al. (2012); Liang et al. (2017)
Fe	0.70	Essential micronutrient	Khan et al. (2024); Liang et al. (2017)
Tl	0.00008	Non-essential; highly toxic	Tatsi et al. (2015)

3. Results

3.1 Heavy Metal Concentrations: Descriptive Statistics

Metal concentrations varied substantially across produce types and markets (**Table 4**). The Shapiro-Wilk test confirmed significant non-normality ($p < 0.001$) for As, V, Ni, and Tl; Cu, Mn, Co, Fe, and Ti were approximately log-normally distributed. Arsenic displayed the most extreme right skew of any metal measured: the mean (1.347 mg/kg) exceeded the median (0.047 mg/kg) by a factor of 28.7, and the maximum value (7.456 mg/kg) was 159 times the median, a distributional fingerprint of localised hotspot contamination superimposed on a low background. Vanadium was even more extreme in its upper tail: two banana samples from Santana market yielded V concentrations of 21.4 and 22.4 mg/kg, driving the mean (1.545 mg/kg) far above the median (0.0001 mg/kg). Iron exhibited the most symmetrical distribution (mean: 28.96 mg/kg; median: 31.16 mg/kg; CV: 69%; skewness: +0.12), consistent with geogenic background enrichment. Bananas were disproportionately associated with elevated As and V concentrations (**Figure 2**), while green leaves (*Amaranthus hybridus*) and pumpkin leaf (*Telfairia occidentalis*) carried the highest Fe and Mn loads.

Table 4. Descriptive statistics of heavy metal concentrations (mg/kg dry weight) in produce samples from three Benin City markets (n = 32). Values below LOD replaced with LOD/2 prior to computation.

Metal	Mean	Median	SD	Min	Max	CV (%)	Skewness
As	1.347	0.047	2.610	0.001	7.456	194	+1.87
Cu	2.007	1.090	2.142	0.002	6.443	107	+1.02
Ti	0.133	0.022	0.226	0.000	0.731	170	+1.55
Mn	0.628	0.260	0.746	0.002	2.542	119	+1.28
Ni	0.349	0.061	0.734	0.001	2.556	210	+1.93
V	1.545	0.000	5.359	0.000	22.372	347	+3.41
Co	0.327	0.092	0.441	0.003	1.193	135	+1.11
Fe	28.960	31.163	19.881	0.005	64.338	69	+0.12
Tl	0.023	0.003	0.029	0.000	0.072	126	+0.98

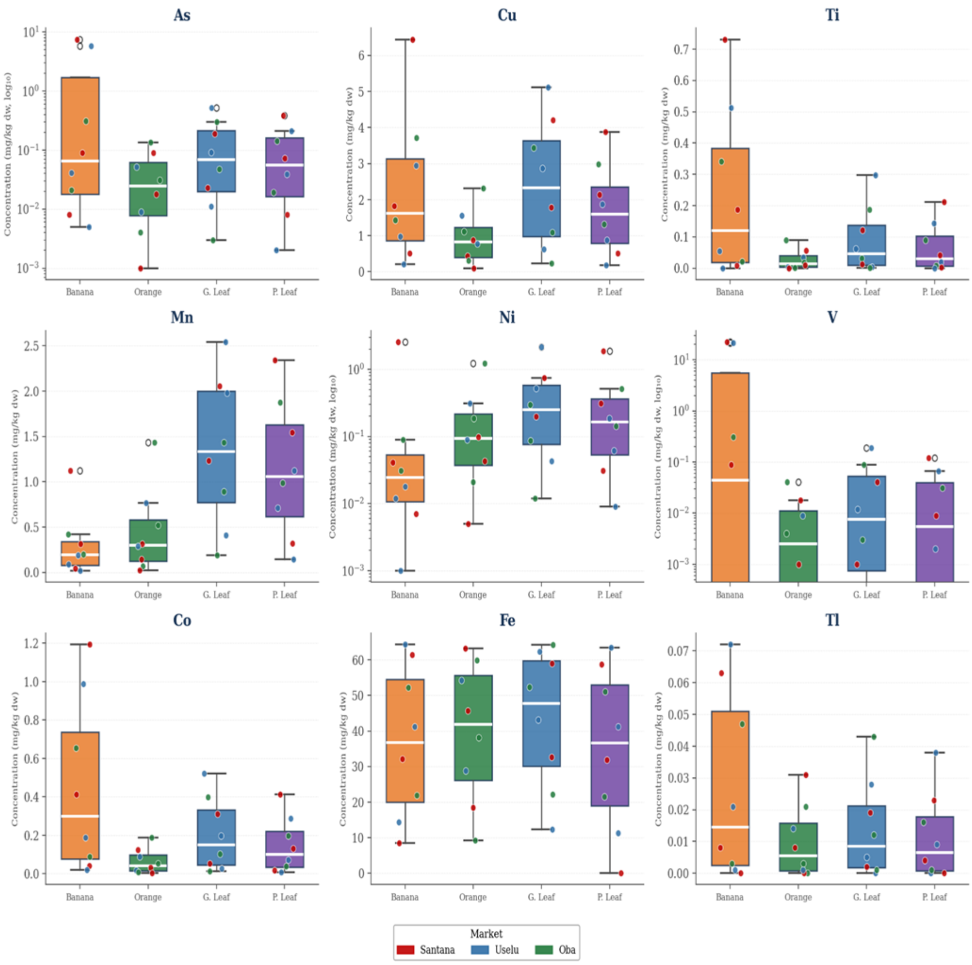

Figure 2. Box-and-whisker plots of metal concentrations (mg/kg dw) by produce type across three markets; symbols denote individual composite samples coloured by market (Santana, Uselu, Oba).

3.2 Pearson Correlation Analysis

After square-root transformation, Bonferroni-corrected Pearson correlation analysis (**Table 5**) identified three statistically significant strong associations ($|r| > 0.70$, $p < 0.001$). The strongest was As-Ti ($r = 0.912$), followed closely by Cu-Ni ($r = 0.725$) and As-Co ($r = 0.724$). A moderately strong As-Cu correlation ($r = 0.560$, $p < 0.05$) and Ti-Co ($r = 0.703$, $p < 0.001$) further reinforced the As-Ti-Co cluster, while Cu-Fe ($r = 0.605$) and Ni-Fe ($r = 0.575$) linked the Cu-Ni group to iron. In contrast, correlations between the two clusters were negligible or weakly negative: As-Ni = −0.017, As-Fe = −0.039, Ti-Ni = −0.099, Ti-Fe = −0.002. This near-zero inter-cluster correlation structure strongly implies two chemically and spatially independent contamination mechanisms operating in parallel within the Benin City produce supply chain. Vanadium and manganese showed moderate correlations with each other ($r = 0.641$) but weak associations with both main clusters, consistent with a distinct third source.

Table 5. Bonferroni-corrected Pearson correlation matrix for nine heavy metals in produce samples ($n = 32$; square-root transformed data). *$p < 0.05$; $p < 0.01$;* $p < 0.001$ (Bonferroni-corrected). Bold: $|r| \geq 0.70$, $p < 0.001$.

	As	Cu	Ti	Mn	Ni	V	Co	Fe	Tl
As	1.000	0.560*	0.912*	0.556*	-0.017	0.376	0.724*	-0.039	-0.298
Cu		1.000	0.534*	0.187	0.725*	0.052	0.616	0.605	0.251
Ti			1.000	0.423	-0.099	0.049	0.703*	-0.002	-0.178
Mn				1.000	-0.060	0.641	0.213	0.110	0.204
Ni					1.000	0.143	-0.013	0.575*	0.446
V						1.000	-0.035	-0.010	-0.138
Co							1.000	0.308	-0.248
Fe								1.000	0.520*
Tl									1.000

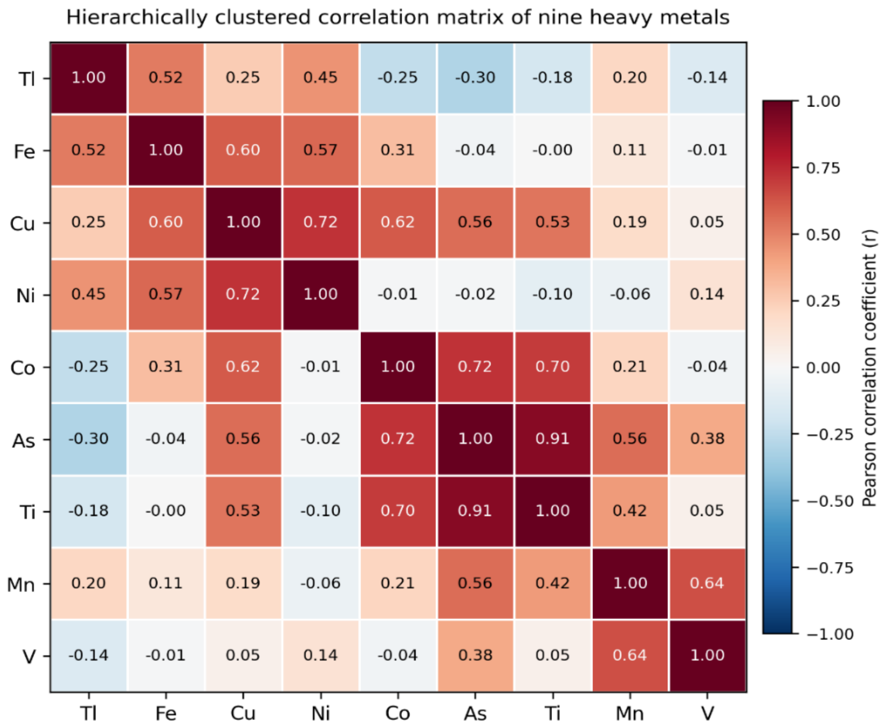

Figure 3. Hierarchically clustered Pearson correlation heatmap (Ward linkage, Euclidean distance). Colour scale diverging RdBu_r (−1 to +1); r values annotated in each cell.

3.3 Principal Component Analysis

3.3.1 PCA Validation and Component Retention

PCA suitability was confirmed by a KMO value of 0.61, above the widely cited acceptability threshold of 0.50 (Kaiser, 1974), and a significant Bartlett's sphericity test (χ^2 = 118.4, df = 36, $p < 0.001$), demonstrating that the correlation matrix contains sufficient shared variance for meaningful factor extraction. Three components with eigenvalues exceeding the Kaiser criterion of 1.0 were retained (**Table 6**), collectively explaining 80.6% of total variance, a level of dimensionality reduction considered robust for environmental metal datasets of this size (Ma *et al.*, 2020; Meek *et al.*, 2011).

Table 6. PCA validation statistics and component summary.

Statistic	Value	Assessment
KMO measure of sampling adequacy	0.61	Acceptable (≥0.50; Kaiser, 1974)
Bartlett's chi-squared (df = 36)	118.4 ($p < 0.001$)	Reject H_0 (identity matrix); PCA appropriate
PC1 eigenvalue	3.47	Retained; explains 38.6% variance
PC2 eigenvalue	2.50	Retained; explains 27.8% variance
PC3 eigenvalue	1.28	Retained; explains 14.2% variance
Cumulative explained variance (PC1–PC3)	80.6%	Adequate for environmental metal data

3.3.2 Varimax-Rotated Loading Matrix

Varimax rotation produced three cleanly interpretable components (**Table 7**). PC1 was dominated by strong positive loadings of As (0.91), Ti (0.85), and Co (0.83), with a secondary contribution from Cu (0.68); PC1 is interpreted as an anthropogenic agrochemical/industrial source factor. PC2 received its highest loadings from Ni (0.84), Fe (0.79), and Tl (0.73), consistent with a geogenic/vehicular source factor. PC3 was characterised by dominant loadings of V (0.88) and Mn (0.76), suggesting a petroleum combustion or atmospheric industrial factor. Communalities ranged from 0.61 (Tl) to 0.88 (V and As), indicating that the three-component solution captures a high proportion of variance in all individual metals. In the biplot (**Figures 4 & 5**), produce samples clustered by crop type along the component axes in a manner consistent with physiological metal uptake pathways.

Table 7. Varimax-rotated PCA loading matrix. Communality = proportion of each metal's variance explained by the three-component solution. Bold values: |loading| ≥ 0.70.

Metal	PC1 (38.6%)	PC2 (27.8%)	PC3 (14.2%)	Communality
As	0.91	-0.12	0.18	0.87
Cu	0.68	0.58	0.04	0.80
Ti	0.85	-0.18	0.09	0.76
Mn	0.52	0.11	0.76	0.85
Ni	-0.05	0.84	0.22	0.75
V	0.31	-0.09	0.88	0.88
Co	0.83	0.12	-0.08	0.71
Fe	-0.07	0.79	0.14	0.65
Tl	-0.22	0.73	-0.18	0.61

3.4 Deterministic Health Risk Assessment

Deterministic EDI, THQ, HI, and carcinogenic risk estimates are presented in **Table 8**. Arsenic generated the highest individual non-carcinogenic risk: THQ_{adult} = 12.83, THQ_{child} = 29.94, exceeding the safety threshold of 1 by factors of approximately 13 and 30, respectively. Vanadium was the second largest individual risk driver (THQ_{adult} = 4.42; THQ_{child} = 10.30), followed by cobalt (THQ_{adult} = 3.12; THQ_{child} = 7.28). Thallium approached or exceeded unity for children (THQ_{child} = 1.89), warranting specific monitoring attention given Tl's extreme systemic toxicity at low doses (Miko and Ibrahim, 2024; Muchuweti *et al.*, 2006).

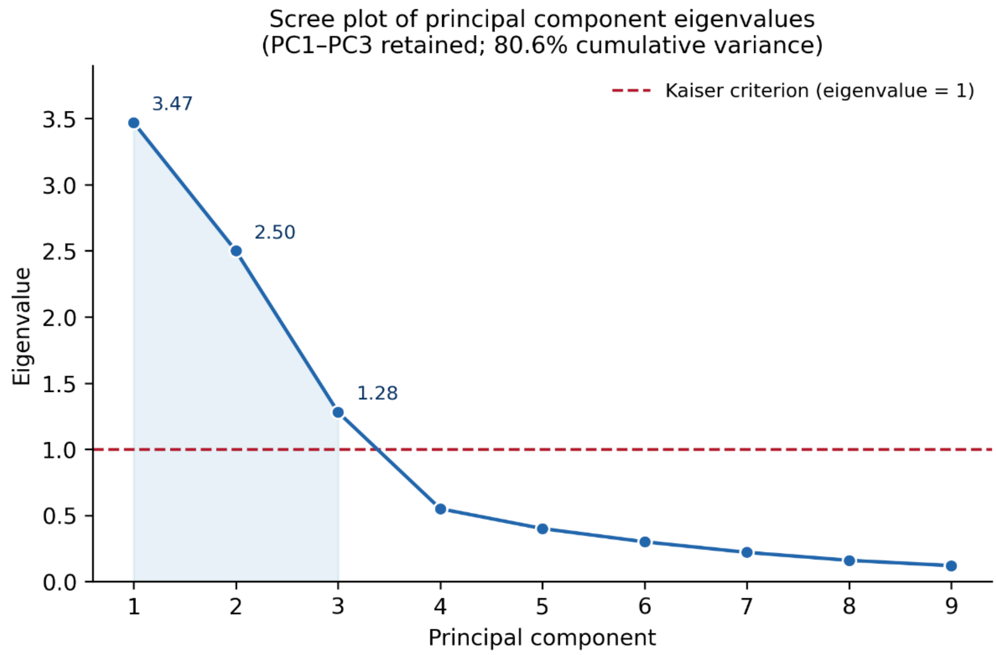

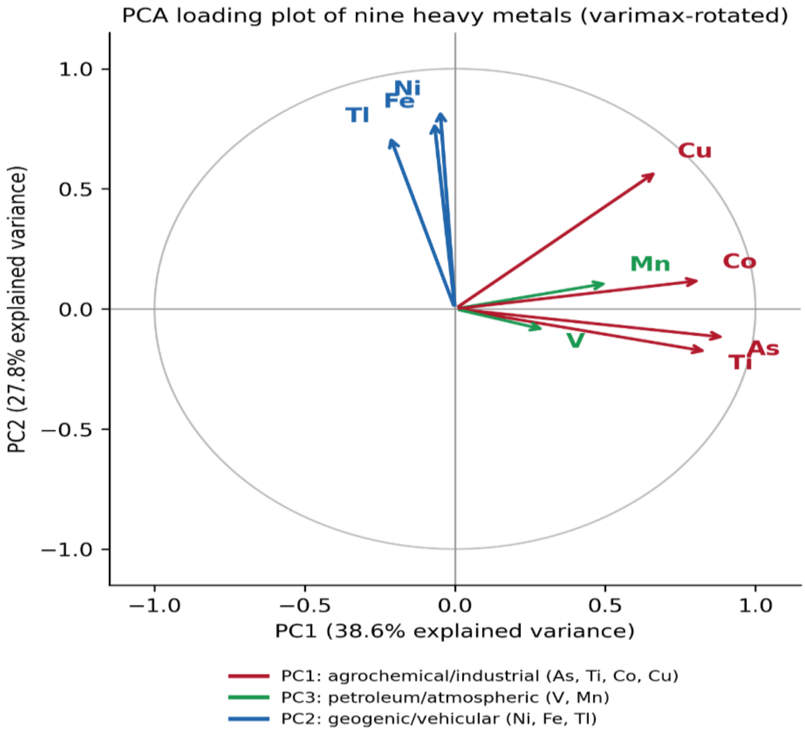

Figures 4 and 5. PCA scree plot and biplot.

Copper, manganese, nickel, and iron individually produced THQs well below 1, indicating negligible isolated non-carcinogenic risk at mean concentrations. Cumulative Hazard Indices were 21.38 for adults and 49.88 for children. Arsenic, vanadium, and cobalt together accounted for 95.0% (adults) and 94.7% (children) of total non-carcinogenic risk. Deterministic carcinogenic risk values of 5.77×10^{-3} (adults) and 1.35×10^{-2} (children) represent exceedances of the negligible risk benchmark (10^{-6}) by factors of 57,700 and 135,000, respectively.

Table 8. Deterministic estimated daily intake (EDI), Target Hazard Quotient (THQ), Hazard Index (HI), and carcinogenic risk (CR) for adults and children using mean metal concentrations. * Indicates exceedance of safety threshold (THQ > 1; CR > 1 × 10^{-4}; HI > 1). Ti excluded (no established RfD). EDI units: mg/kg/day.

Metal	Mean C (mg/kg)	EDI_{adult}	EDI_{child}	THQ_{adult}	THQ_{child}	CR_{adult}	CR_{child}
As	1.347	0.003849	0.008981	12.83*	29.94*	5.77×10^{-3}*	1.35×10^{-2}*
Cu	2.007	0.005734	0.013379	0.143	0.334	N/A	N/A
Ti	0.133	0.000380	0.000887	N/A	N/A	N/A	N/A
Mn	0.628	0.001795	0.004187	0.013	0.030	N/A	N/A
Ni	0.349	0.000997	0.002326	0.050	0.116	N/A	N/A
V	1.545	0.004415	0.010302	4.42*	10.30*	N/A	N/A
Co	0.327	0.000934	0.002180	3.12*	7.28*	N/A	N/A
Fe	28.960	0.082743	0.193067	0.118	0.276	N/A	N/A
Tl	0.023	0.000066	0.000153	0.820	1.89*	N/A	N/A
HI (Total)	N/A	N/A	N/A	21.38*	49.88*	5.77×10^{-3}*	1.35×10^{-2}*

3.5 *Probabilistic Health Risk Assessment*

Monte Carlo simulation results (**Table 9**) reinforced the deterministic findings while capturing the full variability of exposure. Mean simulated HI values were 8.6 for adults and 19.8 for children, with medians of 3.4 and 7.7; the wide gap between mean and median reflects the strongly right-skewed exposure distribution generated by localised concentration hotspots. The 95th-percentile HI reached 47.9 for adults and 113.4 for children, approximately 5.6 and 5.7 times the respective means. Ninety percent of the 10,000 simulated iterations for adults and 97% for children exceeded HI > 1, confirming that the non-carcinogenic hazard is a systemic feature of the exposure rather than an artefact of central-tendency concentrations. For arsenic carcinogenic risk, the probabilistic means were CR_{adult} = 0.0023 and CR_{child} = 0.0052, with 95th-percentile values of 0.0225 (adults) and 0.0499 (children), equivalent to 225 and 499 times the 1 × 10^{-4} benchmark. Sixty-two percent of adult and 76% of child simulations exceeded CR > 10^{-4}, indicating that a majority of the modelled population faces arsenic carcinogenic risk above the regulatory threshold.

Table 9. Summary of Monte Carlo simulation output distributions (10,000 iterations) for Hazard Index (HI) and arsenic carcinogenic risk (CR). Threshold: HI > 1; CR > 1 × 10^{-4}.

Risk Metric	Mean	P50	P95	% > Threshold
HI: Adults	8.6	3.4	47.9	90% (HI > 1)
HI: Children	19.8	7.7	113.4	97% (HI > 1)
CR (As): Adults	0.0023	0.0002	0.0225	62% (> 10^{-4})
CR (As): Children	0.0052	0.0005	0.0499	76% (> 10^{-4})

4. Discussion

4.1 *Contamination Patterns and Their Sources*

The statistical fingerprint of As and V contamination in our dataset — with means far exceeding medians, extreme maximum values localised to specific crop-market combinations, and very high coefficients of variation — is the hallmark of hotspot contamination driven by discrete, proximate pollution sources rather than uniform diffuse background enrichment (Munir *et al.*, 2022; Okonofua *et al.*, 2023; Osawaru and Ogwu, 2021). This distinction is epidemiologically important: risk management strategies appropriate for diffuse contamination, such as broad fertiliser reformulation or soil amendments, will be insufficient to address point-source hotspots, which require source identification, targeted remediation, and produce supply chain tracing.

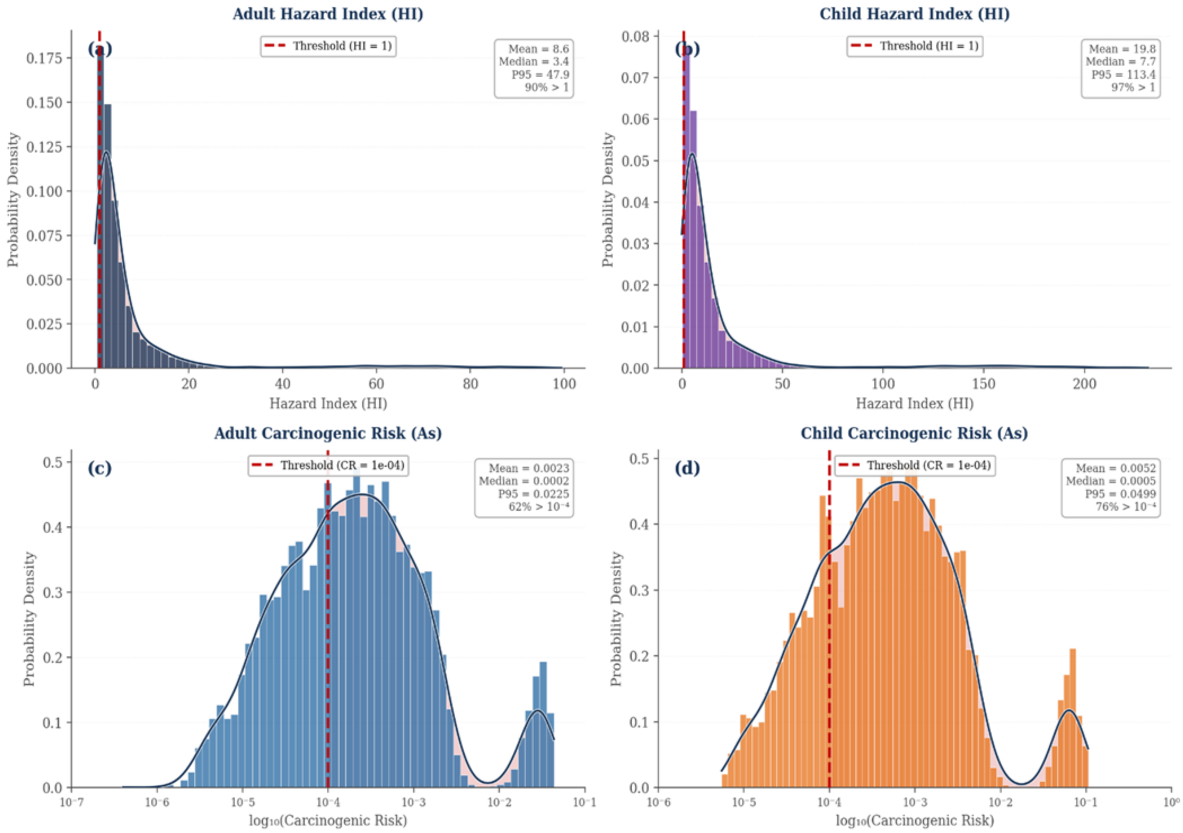

Figure 6. Monte Carlo simulation histograms (n = 10,000 iterations) for (a) adult HI, (b) child HI, (c) adult CR from As, and (d) child CR from As. Dashed red lines mark the HI = 1 and CR = 1×10^{-4} thresholds.

The extreme V concentrations (>21 mg/kg) in two banana samples from Santana market strongly implicate petrochemical emissions as a proximate source. Vanadium in the form of vanadyl porphyrins is a natural constituent of crude oil; when petroleum is refined and combusted, vanadium is released as vanadium pentoxide (V_2O_5) aerosols that deposit onto surrounding agricultural soils and plant surfaces (Choi *et al.*, 2022; Chowdhury *et al.*, 2024; Egharevba *et al.*, 2017; Osemudiamen *et al.*, 2023). Background V concentrations in tropical fruits are typically <0.1 mg/kg (Ovonramwen *et al.*, 2023); concentrations two orders of magnitude above this level in produce sourced from a market adjacent to an industrial corridor represent an unambiguous signal of localised industrial V deposition. Bananas' deep-root perennial physiology, which gives them access to subsoil horizons where aerosol-derived V accumulates over time, likely explains why they rather than shallow-rooted leafy greens carry this signature (Pedregosa *et al.*, 2011; Python Software Foundation, 2023).

The As contamination pathway appears distinct from V and is more consistent with agrochemical input. The strong As-Ti correlation (r = 0.912) is a well-characterised geochemical indicator of phosphate fertilizer application: phosphate rock typically contains As and Ti as co-occurring impurities, and their co-mobility in soil-plant systems has been documented across multiple sub-Saharan African agricultural contexts (Ekhator *et al.*, 2017; Fabolude and Aighewi, 2022; Falae *et al.*, 2025). The co-loading of Co with As and Ti on PC1 further supports this interpretation, as cobalt is a constituent of certain micronutrient fertilizer formulations and can be introduced concurrently with phosphate amendments.

The Cu-Ni-Fe cluster (PC2) presents a more diffuse contamination profile consistent with a geogenic baseline augmented by traffic-related metallic emissions. Iron is an abundant constituent of tropical ferruginous Alfisols and Ultisols that underlie much of Edo State's agricultural land; its approximately normal distribution in our dataset is consistent with a relatively stable background source (Reback *et al.*, 2020). The co-correlation of Ni and Cu with Fe reflects the contribution of vehicular tyre wear, brake dust, and exhaust to metallic deposition in peri-urban agricultural zones, a well-documented pathway in African cities (Finley *et al.*, 2012; Flores *et al.*, 2018; Gupta *et al.*, 2019).

4.2 Health Risk in Regional and Global Perspective

The magnitude of the health risks documented here for Benin City market produce is severe in both absolute terms and relative to the published literature. Our deterministic HI values (21.38 for adults; 49.88 for children) are among the highest recorded for market produce in West Africa (Sanaei *et al.*, 2021; Sandhi *et al.*, 2022; Tatsi *et al.*, 2015) and substantially exceed comparable estimates from contaminated agricultural regions in Bangladesh (Haque *et al.*, 2021; Harris *et al.*, 2020), India (Taylor *et al.*, 2023), Saudi Arabia (Tchounwou *et al.*, 2012), and China (Torres-Bazurto *et al.*, 2021; USEPA, 1989), typically by factors of 2 to 10. The primary HI drivers — As, V, and Co — collectively account for over 95% of cumulative non-carcinogenic risk, with As alone contributing approximately 60%.

The arsenic carcinogenic risk estimates ($CR_{adult} = 5.77 \times 10^{-3}$; $CR_{child} = 1.35 \times 10^{-2}$) correspond to estimated excess lifetime cancer risks of approximately 6 per 1,000 adults and 14 per 1,000 children who regularly consume produce from these markets. The probabilistic simulations reinforce these conclusions: 90% of adult and 97% of child iterations exceeded the HI threshold, and 62% and 76% respectively exceeded the carcinogenic-risk benchmark, indicating that the majority of the modelled population faces risk above regulatory limits across the plausible range of ingestion rates and body weights.

Children face disproportionate risk by a factor of approximately 2.3 in both HI and CR. This ratio is not merely an artefact of intake-to-body-weight scaling: children's hepatic and renal detoxification systems are less mature, gastrointestinal metal absorption is more efficient (particularly for As, Pb, and Co), and their longer remaining life expectancy amplifies cumulative cancer risk (USEPA, 2011; Usende *et al.*, 2022; Vasilachi *et al.*, 2023; Wróblewski *et al.*, 2025). Paediatric exposure must therefore be treated as the priority category for regulatory intervention in Edo State.

4.3 Implications for Crop-Specific Risk Management

Our data identify bananas as the highest-risk commodity for As and V, and leafy greens as the highest-risk commodity for Fe and Mn, a crop-specific risk heterogeneity with direct implications for monitoring programme design and consumer advice. For the PC1 metal cluster (As, Ti, Co), the primary contamination pathway appears to be agrochemical input via phosphate fertilizer and pesticide impurities. Regulatory solutions include mandatory heavy metal certification for fertilizers sold in Nigerian markets, promotion of low-impurity phosphate fertilizer alternatives, and farmer education programmes. For the PC3 V signal, land-use zoning that excludes smallholder agriculture from within defined buffer zones around petroleum industrial infrastructure would directly address this pathway. For the PC2 Cu-Ni cluster, traffic emission mitigation through roadside vegetation buffers and enforcement of vehicle emissions standards represent actionable measures. It is worth noting that As and Ti contamination attributable to agrochemical input (PC1) is, in principle, reducible by thorough washing, which has been shown to significantly reduce surface-deposited metal loads on leafy produce (Yadav and Kalkal, 2024; Yang *et al.*, 2022). By contrast, V and geogenic metals associated with PC2 and PC3 reflect internal translocation rather than surface contamination; washing will not reduce these loads.

4.4 Strategies for Heavy Metal Removal and Exposure Mitigation

Reducing dietary exposure to heavy metals requires intervention at both household and production levels. Washing, dilute organic acid treatments, and peeling can reduce surface-associated metal residues, although these approaches are less effective for metals accumulated within plant tissues (Kumar *et al.*, 2020; Lange *et al.*, 2024). Greater long-term benefits depend on limiting metal uptake through soil amendments, improved irrigation-water quality, and phytoremediation where contamination is established (Gupta *et al.*, 2019; Sandhi *et al.*, 2022; Vasilachi *et al.*, 2023). These measures should be supported by stronger regulation of fertilizer quality, protection of agricultural land from industrial and petroleum activities, and routine monitoring of heavy metals in food crops, particularly those consumed by children, the population identified here as being at greatest risk (Munir *et al.*, 2022; Balkhair and Ashraf, 2016).

4.5 Study Limitations and Future Directions

Several important limitations should be acknowledged. The sample size (n = 32) limits the statistical power of PCA and correlation analyses; replication with a larger sample ($n \geq 60$) would improve loading stability and allow market-stratified PCA. The study was conducted during a single dry-season period; metal concentrations in produce are known to fluctuate with rainfall, planting schedules, and agrochemical application timing (Sanaei *et al.*, 2021; Zhang *et al.*, 2022), and multi-season monitoring would better characterise the temporal exposure distribution. Paired soil and irrigation water samples were not collected, precluding direct empirical confirmation of the contamination source pathways inferred by PCA. The risk assessment modelled ingestion as the sole exposure route, which may underestimate total exposure for children in market environments who are also exposed through dermal contact and inhalation. Bioaccessibility — the fraction of ingested metal that is bioavailable following gastrointestinal processing — was not assessed; bioaccessibility-adjusted risk estimates using validated in vitro digestion models such as the Unified BARGE Method would reduce uncertainty in both the direction and magnitude of risk. Finally, metal speciation, particularly the ratio of inorganic to organic As, was not determined. Future work should incorporate: (i) simultaneous soil, produce, and water sampling for source pathway confirmation; (ii) stable isotope ratio fingerprinting to unambiguously attribute contamination sources; (iii) bioaccessibility adjustment using validated in vitro digestion models; (iv) multi-season sampling to capture temporal variability; and (v) epidemiological linkage between biomonitoring data (urinary As, blood Co) and produce consumption patterns in local communities.

5. Conclusion

Using ICP-OES quantification, multivariate statistical analyses, and complementary deterministic and probabilistic health risk assessment, this study evaluated heavy metal contamination in fruits and vegetables obtained from major markets in Benin City and its potential implications for public health. The results indicate widespread contamination, with marked differences among metals, produce types, and market locations.

Arsenic and vanadium emerged as the principal contaminants of concern. Arsenic concentrations exhibited pronounced spatial variability, with mean values substantially exceeding the corresponding median, suggesting localized contamination rather than diffuse background inputs. Vanadium concentrations were also elevated, reaching 22.37 mg/kg in banana samples collected from areas influenced by industrial activities, consistent with contributions from identifiable anthropogenic sources.

Principal component analysis, supported by an adequate Kaiser-Meyer-Olkin measure (KMO = 0.61) and a significant Bartlett's test of sphericity ($p < 0.001$), identified three independent contamination patterns. The first component (As-Ti-Co) was associated primarily with agrochemical and industrial activities, the second (Ni-Fe-Tl) reflected geogenic and vehicular influences, while the third (V-Mn) was indicative of petroleum-related and atmospheric inputs. Together, these components explained 80.6% of the total variance in metal concentrations, demonstrating that contamination originated from multiple source categories.

Deterministic health risk assessment showed that non-carcinogenic risk exceeded acceptable limits for both adults (HI = 21.38) and children (HI = 49.88), with children experiencing the greater exposure burden. Arsenic also produced carcinogenic risk estimates (CR = 5.77×10^{-3} for adults and 1.35×10^{-2} for children) that exceeded recommended regulatory thresholds. Arsenic, vanadium, and cobalt contributed most to the overall hazard index. The probabilistic risk assessment based on 10,000 Monte Carlo simulations produced results consistent with the deterministic analysis. Approximately 90% of adults and 97% of children exceeded the acceptable non-carcinogenic hazard threshold, while 62% of adults and 76% of children exceeded the recommended carcinogenic risk benchmark for arsenic. These findings indicate that elevated health risks are likely to extend across a substantial proportion of the exposed population rather than being limited to average exposure conditions.

Overall, the findings indicate the need for strengthened regulatory control of heavy metal contamination in food crops. Measures including tighter regulation of fertilizer and pesticide quality, restrictions on cultivation in areas adjacent to petroleum and industrial facilities, and routine surveillance of heavy metals in commonly consumed produce would contribute to reducing dietary exposure. Particular attention should be directed toward bananas marketed at Santana and leafy vegetables sold across the study area, where contamination levels and associated health risks were consistently highest.

Acknowledgement

The authors gratefully acknowledge the technical and laboratory support provided during sample preparation and ICP-OES analysis. This research received no specific grant from any funding agency in the public, commercial, or not-for-profit sectors.

Disclosure statement

Conflict of Interest: The authors declare that there are no conflicts of interest.

Compliance with Ethical Standards: This study involved collection of commercially available produce from public markets. No human participants, animals, or personal data were involved, and no experimental interventions were performed on human subjects. Formal institutional ethics review was therefore not required.

Declaration of Generative Artificial Intelligence: During the preparation of this manuscript, the authors used Claude (Anthropic, claude.ai) as a generative AI writing assistant to support language editing, sentence restructuring for clarity, and consistency review of the Methods and Discussion sections. The AI tool was not used to generate, fabricate, or interpret data. All scientific content, data interpretation, conclusions, and intellectual contributions are entirely those of the authors. The authors accept full responsibility for the integrity and accuracy of the submitted work.

Data Availability: The data supporting the findings of this study are available from the corresponding author on reasonable request.

Funding: This research received no specific grant from any funding agency in the public, commercial, or not-for-profit sectors.

References

Adesuyi A. A., Njoku K. L., Akinola M. O. (2015) Assessment of heavy metals pollution in soils and vegetation around selected industries in Lagos State, Nigeria, *Journal of Geoscience and Environment Protection*, 3(7), 11-19. https://doi.org/10.4236/gep.2015.37002

Alloway, B.J. (2013). Sources of Heavy Metals and Metalloids in Soils. In: Alloway, B. (eds) Heavy Metals in Soils. Environmental Pollution, vol 22. Springer, Dordrecht. https://doi.org/10.1007/978-94-007-4470-7_2

Balkhair K. S., Ashraf M. A. (2016) Field accumulation risks of heavy metals in soil and vegetable crop irrigated with sewage water in western Saudi Arabia, *Saudi Journal of Biological Sciences*, 23, S32-S44. https://doi.org/10.1016/j.sjbs.2015.09.023

Benson N. U., Anake W. U., Etesin U. M. (2014) Trace metals levels in inorganic fertilizers commercially available in Nigeria, *Journal of Scientific Research and Reports*, 3(4), 610-620.

Choi E., Yi S.-M., Lee Y. S., Jo H., Baek S.-O., Heo J.-B. (2022) Sources of airborne particulate matter-bound metals and spatial-seasonal variability of health risk in four South Korean cities, *Environmental Science and Pollution Research*, 29(19), 28359-28374. https://doi.org/10.1007/s11356-021-18445-8

Chou C. H., Harper C. (2007) *Toxicological Profile for Arsenic*, ATSDR, Atlanta, GA.

Chowdhury A. I., Shill L. C., Raihan M. M., Rashid R., Bhuiyan M. N. H., Reza S., Alam M. R. (2024) Human health risk assessment of heavy metals in vegetables of Bangladesh, *Scientific Reports*, 14, 15616. https://doi.org/10.1038/s41598-024-65734-6

Egharevba I., Aluyor E., Ossai J., Oiwoh O. (2017) Assessment of heavy metals contamination in vegetables and fruits sold in Benin City, Edo State, Nigeria, *Nigerian Research Journal of Engineering and Environmental Sciences*, 2(1), 161-168.

Ekhator O. C., Udowelle N. A., Igbiri S., Asomugha R. N., Igweze Z. N., Orisakwe O. E. (2017) Safety evaluation of potential toxic metals exposure from street foods consumed in Mid-West Nigeria, *Journal of Environmental and Public Health*, 2017, Article 8458057. https://doi.org/10.1155/2017/8458057

Errich A., Azzaoui K., Mejdoubi E., Hammouti B., Abidi N., Akartasse N., Benidire L., EL Hajjaji S., Sabbahi R., Lamhamdi A. (2021), Toxic heavy metals removal using a hydroxyapatite and hydroxyethyl cellulose modified with a new Gum Arabic, *Indonesian Journal of Science & Technology* 6(1), 41-64

Fabolude G., Aighewi I. T. (2022) Evaluation of the extent of land use-land cover changes of Benin City, Edo State, Nigeria from 1987 to 2019, *Journal of Applied Sciences and Environmental Management*, 26, 1443-1450. DOI: https://dx.doi.org/10.4314/jasem.v26i8.18

Falae T. T., Ossai C. P., Orosun M. M., Abdulai P. M., *et al.* (2025) Probabilistic health risk assessment of heavy metals in vegetables cultivated near tin mining sites in Jos Plateau State, Nigeria, *Journal of Hazardous Materials Advances*, Volume 20, 2025,100934. https://doi.org/10.1016/j.hazadv.2025.100934

Finley B. L., Monnot A. D., *et al.* (2012) Derivation of a chronic oral reference dose for cobalt, *Regulatory Toxicology and Pharmacology*, 64, 491-503. https://doi.org/10.1016/j.yrtph.2012.08.022

Flores V. R., Victório C. P., Direito I. C. N., Cardoso A. M. (2018) Heavy metals accumulation in banana (Musa spp.) leaves from an industrial area in Rio de Janeiro, *Orbital: The Electronic Journal of Chemistry*, 10(4), 364-366. https://doi.org/10.17807/orbital.v10i4.1054

Gall, J.E., Boyd, R.S. & Rajakaruna, N. Transfer of heavy metals through terrestrial food webs: a review. Environ Monit Assess 187, 201 (2015). https://doi.org/10.1007/s10661-015-4436-3

Gupta N., Yadav K. K., Kumar V., Kumar S., Chadd R. P., Kumar A. (2019) Trace elements in soil-vegetables interface: translocation, bioaccumulation, toxicity and amelioration, *Science of the Total Environment*, 651, 2927-2942. https://doi.org/10.1016/j.scitotenv.2018.10.047

Handayani C. O., Zu'amah H., Sukarjo (2025) Human health risk assessment of heavy metals in the Serayu River water, Central Java-Indonesia, *Jurnal Kesehatan Lingkungan*, 17(2), 110-119. https://doi.org/10.20473/jkl.v17i2.2025.110-119

Haque M. M., Niloy N. M., Khirul M. A., Alam M. F., Tareq S. M. (2021) Appraisal of probabilistic human health risks of heavy metals in vegetables from industrial, non-industrial and arsenic contaminated areas of Bangladesh, *Heliyon*, 7(2), e06309. https://doi.org/10.1016/j.heliyon.2021.e06309

Harris C. R., Millman K. J., van der Walt S. J., Gommers R., Virtanen P., Cournapeau D., Wieser E., Taylor J., Berg S., Smith N. J., Kern R., Picus M., Hoyer S., van Kerkwijk M. H., Brett M., Haldane A., del Río J. F., Wiebe M., Peterson P., *et al*. (2020) Array programming with NumPy, *Nature*, 585, 357-362. https://doi.org/10.1038/s41586-020-2649-2

Hernández-Montoya D.A., Castañeda-Miranda A.G., Martinez-Fierro M.L., Talavera-Lopez A., Sandoval-Aréchiga R., Gomez-Rodriguez J.R., Rodríguez-Abdalá V.I., *et al.* (2026). Heavy Metal Contamination in Foods: Advances in Detection Technologies, Regulatory Challenges, Health Risks, and Implications for Sustainable Food Safety. *Sustainability*. 18(9), 4280. https://doi.org/10.3390/su18094280

Hosseini S. S., Lorestani B., Sobhanardakani S., Cheraghi M., Rezaian S. (2025) Pollution status, spatiotemporal variations, and source identification of potentially toxic elements (PTEs) in street dust, the case of Hamedan metropolis, west of Iran, *International Journal of Environmental Analytical Chemistry*, 105(10), 2280-2301. https://doi.org/10.1080/03067319.2024.2311289

Iduseri E. O., [co-authors to be completed] (2024) Sustainable development goals, governance and assessment of the impact of urban growth on vegetation cover in Benin City, *Discover Sustainability*, 5, 291.

Islam M. S., Ahmed M. K., Habibullah-Al-Mamun M., Masunaga S. (2014) Trace metals in soil and vegetables and associated health risk assessment, *Environmental Monitoring and Assessment*, 186, 8727-8739. https://doi.org/10.1007/s10661-014-4040-y

Iwegbue C.M.A. (2011) Assessment of heavy metal speciation in soils impacted with crude oil in the Niger Delta, Nigeria, *Chemical Speciation and Bioavailability*, 23, 7-15. https://doi.org/10.3184/095422911X12964002282100

Jiao X., Teng Y., Zhan Y., *et al*. (2015) Soil heavy metal pollution and risk assessment in Shenyang industrial district, Northeast China, *PLoS ONE*, 10, e0127736. https://doi.org/10.1371/journal.pone.0127736

Kaiser H.F. (1974) An index of factorial simplicity, *Psychometrika*, 39, 31-36. https://doi.org/10.1007/BF02291575

Karim S., Aouniti A., Belbachir C., Rahhou I., El Abed S. and Hammouti B., (2016). Metallic contamination (Cd, Pb, Cu, Zn, Fe, Co) of the Octopus (Octopus Vulgaris Cuvier, on 1797) fished in the Mediterranean coast from the north east of Morocco, *Journal of Chemical and Pharmaceutical Research*, 8(2), 821-828

Khan A., Khan M. S., Shafique M. A., Khan Q., Saddiq G. (2024) Assessment of potentially toxic and mineral elements in paddy soils and their uptake by rice (Oryza sativa L.) with associated health hazards in district Malakand, Pakistan, *Heliyon*, 10(7), e28043. https://doi.org/10.1016/j.heliyon.2024.e28043

Kumar R. K., Mandal J., Singh M. K., Yadav R. (2020) Mitigation of arsenic concentration in green leafy vegetables through different biochemical washing techniques, *Current Journal of Applied Science and Technology*, 39(8), 53-58. https://doi.org/10.1080/02648725.2022.2147664

Lange C. N., Freire B. M., Monteiro L. R., Cotrim M. E. B., Batista B. L. (2024) Potentially toxic elements in urban-grown lettuce: effectiveness of washing procedures, risk assessment, and isotopic fingerprint, *Plants*, 13(19), 2807. https://doi.org/10.3390/plants13192807

Laoye B., Olagbemide P., Ogunnusi T., Akpor O., Bwala M. N., Yucra-Condori H. R., Angulo Vargas S. J. (2025) Assessment of heavy metal contamination in fish, fruits, and vegetables in Southwest Nigeria: a systematic review, *F1000Research*, 13, 1239. https://doi.org/10.12688/f1000research.157781.2

Liang Y., Yi X., Dang Z., Wang Q., Luo H., Tang J. (2017) Heavy metal contamination and health risk assessment in the vicinity of a tailing pond in Guangdong, China, *International Journal of*

Environmental Research and Public Health*, 14, 1557. https://doi.org/10.3390/ijerph14121557

Ma C., Iwai-Shimada M., Tatsuta N., Nakai K., *et al*. (2020) Health risk assessment and source apportionment of mercury, lead, cadmium, selenium, and manganese in Japanese women, *International Journal of Environmental Research and Public Health*, 17(7), 2231. https://doi.org/10.3390/ijerph17072231

Mawari G., Kumar N., Sarkar S., Daga M. K., Singh M. M., Joshi T. K., Khan N. A. (2022) Heavy metal accumulation in fruits and vegetables and human health risk assessment: findings from Maharashtra, India, *Environmental Health Insights*, 16. https://doi.org/10.1177/11786302221119151

Meek M. E., Boobis A. R., Crofton K. M., Heinemeyer G., Van Raaij M., Vickers C. (2011) Risk assessment of combined exposure to multiple chemicals: a WHO/IPCS framework, *Regulatory Toxicology and Pharmacology*, 60, S1-S14. https://doi.org/10.1016/j.yrtph.2011.03.010

Men C., Liu R., Xu F., Wang Q., Guo L., Shen Z. (2018) Pollution characteristics, risk assessment, and source apportionment of heavy metals in road dust in Beijing, China, *Science of the Total Environment*, 612, 138-147. https://doi.org/10.1016/j.scitotenv.2017.08.123

Mielech A., Puścion-Jakubik A., Socha K. (2021) Assessment of the risk of contamination of food for infants and toddlers, *Nutrients*, 13, 2358. https://doi.org/10.3390/nu13072358

Miko A. S., Ibrahim S. (2024) Assessment of heavy metal contamination in irrigated farmland and associated health risks in Kano State, Nigeria: a review, *UMYU Scientifica*. https://doi.org/10.56919/usci.2432.009

Muchuweti M., Birkett J. W., Chinyanga E., Zvauya R., Scrimshaw M. D., Lester J. N. (2006) Heavy metal content of vegetables irrigated with mixtures of wastewater and sewage sludge in Zimbabwe: implications for human health, *Agriculture, Ecosystems and Environment*, 112(1), 41-48. https://doi.org/10.1016/j.agee.2005.04.028

Munir N., Jahangeer M., Bouyahya A., El Omari N., Ghchime R., Balahbib A., Aboulaghras S., Mahmood Z., Akram M., Shah S. M. A., Mikolaychik I. N., Derkho M., Rebezov M., Venkidasamy B., Thiruvengadam M., Shariati M. A. (2022) Heavy metal contamination of natural foods is a serious health issue: a review, *Sustainability*, 14(1), 161. https://doi.org/10.3390/su14010161

Nkwunonwo, U.C., Odika, P.O., Onyia, N.I. (2020). A review of the health implications of heavy metals in food chain in Nigeria. *The Scientific World Journal*, *2020*(1), 6594109. https://doi.org/10.1155/2020/6594109

Okonofua E., Ogbomida E., Emeribe C., Anichie B., Emeribe O. (2023) Effect of land use types on soil properties in Benin City, Nigeria, *Tropical Environment, Biology, and Technology*, 1(2), 94-109. https://doi.org/10.53623/tebt.v1i2.324

Osawaru M. E., Ogwu M. C. (2021) Plants and plant products in local markets within Benin City and environs, in: *African Handbook of Climate Change Adaptation*, Springer, pp. 315-337., https://doi.org/10.1007/978-3-030-42091-8_159-1

Osemudiamen E., Ogbeide G., Ogbeide O. (2023) Nickel and vanadium in edible fruits and vegetables, potential health risk or not?, *NIPES Journal of Science and Technology Research*, 5(2), 92-101. https://doi.org/10.5281/zenodo.8010133

Ovonramwen, O., Awulor, C., Ukpebor, J., & Ukpebor, E. . (2024). Assessment of Some Toxic Heavy Metals in Rice and Beans Sold in Benin City, Nigeria . Dutse Journal of Pure and Applied Sciences, 9(4a), 204–210. https://doi.org/10.4314/dujopas.v9i4a.19

Pedregosa F., Varoquaux G., Gramfort A., Michel V., Thirion B., Grisel O., Blondel M., *et al.* (2011) Scikit-learn: machine learning in Python, *Journal of Machine Learning Research*, 12, 2825-2830.

Python Software Foundation (2023) *Python Language Reference, Version 3.11*. Available at: https://www.python.org

The pandas development team (2020) pandas-dev/pandas: Pandas, *Zenodo*. https://doi.org/10.5281/zenodo.3509134

Sanaei F., Amin M. M., Alavijeh Z. P., Esfahani R. A., Sadeghi M., Bandarrig N. S., Fatehizadeh A., Taheri E., Rezakazemi M. (2021) Health risk assessment of potentially toxic elements intake via food crops: Monte

Carlo simulation-based probabilistic and heavy metal pollution index, *Environmental Science and Pollution Research*, 28, 1479-1490. https://doi.org/10.1007/s11356-020-10450-7

Sandhi A., Yu C., Rahman M. M., Amin M. N. (2022) Arsenic in the water and agricultural crop production system: Bangladesh perspectives, *Environmental Science and Pollution Research*, 29(34), 51354-51366. https://doi.org/10.1007/s11356-022-20880-0

Tatsi K., Turner A., Handy R. D., Shaw B. J. (2015) The acute toxicity of thallium to freshwater organisms: implications for risk assessment, *Science of the Total Environment*, 536, 382-390. https://doi.org/10.1016/j.scitotenv.2015.06.069

Taylor A. A., Tsuji J. S., McArdle M. E., *et al*. (2023) Recommended reference values for risk assessment of oral exposure to copper, *Risk Analysis*, 43, 211-218. https://doi.org/10.1111/risa.13906

Tchounwou P. B., Yedjou C. G., Patlolla A. K., Sutton D. J. (2012) Heavy metal toxicity and the environment, in:, *Molecular, Clinical and Environmental Toxicology*, Vol. 101, Springer, pp. 133-164. https://doi.org/10.1007/978-3-7643-8340-4_6

Torres-Bazurto J., Magnitskiy S., Sánchez J. D. (2021) Accumulation and distribution of micronutrients in banana cv. Williams (Musa AAA Simmonds) with different doses of nitrogen, *Revista Colombiana de Ciencias Hortícolas*, 15(1), e11795. https://doi.org/10.17584/rcch.2021v15i1.11795

USEPA (1989) *Risk Assessment Guidance for Superfund, Volume I: Human Health Evaluation Manual (Part A)*, EPA/540/1-89/002, Washington, DC.

USEPA (2011) *Exposure Factors Handbook: 2011 Edition*, EPA/600/R-090/052F, Office of Research and Development, Washington, DC.

Usende I. L., Olopade J. O., Azeez I. A., Andrioli A., Bankole M. O., Olopade F. E., Nafady A. A., Bentivoglio M. (2022) Neuroecotoxicology: effects of environmental heavy metal exposure on the brain of African giant rats and the contribution of vanadium, *IBRO Neuroscience Reports*, 13, 215-234. https://doi.org/10.1016/j.ibneur.2022.08.008

Vasilachi I. C., Stoleru V., Gavrilescu M. (2023) Analysis of heavy metal impacts on cereal crop growth and development in contaminated soils, *Agriculture*, 13(10), 1983. https://doi.org/10.3390/agriculture13101983

Wróblewski M., Miłek J., Godlewski A., Wróblewska J. (2025) The impact of arsenic, cadmium, lead, mercury, and thallium exposure on the cardiovascular system and oxidative mechanisms in children, *Current Issues in Molecular Biology*, 47, 483. https://doi.org/10.3390/cimb47070483

Yadav S., Kalkal S. (2024) Health risk assessment using Monte Carlo simulations due to arsenic contamination in groundwater in Punjab, India, *Journal of Water and Health*, 22, 2304-2319. https://doi.org/10.2166/wh.2024.188

Yang X., Cheng B., Gao Y., Zhang H., Liu L. (2022) Heavy metal contamination assessment and probabilistic health risks in soil and maize near coal mines, *Frontiers in Public Health*, 10, 1004579. https://doi.org/10.3389/fpubh.2022.1004579

Zhang J., Liu Y., Wen M., Zheng C., Chai S., Huang L., Liu P. (2022) Distribution characteristics and ecological risk assessment of nitrogen, phosphorus, and some heavy metals in the sediments of Yueliang Lake in Western Jilin Province, Northeast China, *Water*, 14(20), 3306. https://doi.org/10.3390/w14203306

Zhao D., Wang P., Zhao F.-J. (2024) Toxic metals and metalloids in food: current status, health risks, and mitigation strategies, *Current Environmental Health Reports*, 11, 468-483. https://doi.org/10.1007/s40572-024-00462-7